SEECCM III
3rd South-East European Conference on Computational Mechanics-
an ECCOMAS and IACM Special Interest Conference
M. Papadrakakis, M. Kojic, I. Tuncer (eds.)
Kos Island, Greece, 12–14 June 2013

GENERATING EMBEDDED REBAR ELEMENTS FOR LARGE-SCALE RC MODELS

George Markou[1] and Manolis Papadrakakis[2]

[1]Department of Civil Engineering, Alhosn University, Abu Dhabi, UAE
P.O.Box 38772, Abu Dhabi
g.markou@alhosnu.ae

[2]Department of Civil Engineering, National Technical University of Athens
GR-15780 Athens, Greece
mpapadra@cental.ntua.gr

Keywords: Embedded Reinforcement, Mesh Generation, Large-Scale Models.

Abstract. *Modeling of reinforced concrete structures through the use of 3D detailed models derives significant numerical issues especially when dealing with large-scale meshes that incorporate large numbers of reinforcement bars embedded in the hexahedral mesh. In 3D detailed reinforced concrete simulations, mapping the reinforcement grid inside the concrete hexahedral finite elements is performed by using the end-point coordinates of the rebar macro-elements. This procedure is computationally demanding when dealing with large-scale models, where the required computational time for the reinforcement mesh generation can be excessive. This research work investigates the numerical robustness and computational efficiency of the embedded rebar mesh generation method proposed by Markou [14] that was an extension of the Markou and Papadrakakis [8] research work. The under study embedded rebar mesh generation method foresees the automatic allocation and generation of embedded steel reinforcement inside hexahedral finite elements for 32-bit and 64-bit windows based applications. In order to investigate the numerical and computational performance of the embedded rebar mesh generation method, a full-scale model of the RC frame of the Alhosn University Campus in Abu Dhabi and a RC bridge are constructed and used so as to allocate and generate the embedded rebar finite elements. The numerical results that derived from the ReConAn FEA solver for the at hand numerical implementations are briefly presented.*

1 INTRODUCTION

Modeling of reinforced concrete (RC) structures with the use of 3D detailed models is usually performed by research teams [1-5] or by large consultancy companies [6-7] that foresee the thorough investigation of the mechanical behavior of geometrically complicated RC structures. Researchers have been using this modeling type so as to verify experimental results or develop new constitutive models in an attempt to derive a numerically objective modeling method that will eventually provide the ability of performing assessment analysis for any type of RC structure geometry and design.

As it was described in [8], when modeling 3D RC structures with the finite element (FE) method, three main approaches are available for the simulation of reinforcement: smeared, discrete, and embedded [9-11]. The smeared and discrete formulations have been found to be unsuitable for complicated reinforcement grid geometries thus undergo several restrictions when implemented. On the other hand, the embedded reinforcement formulation provides the ability of representing the grid's geometry in an exact manner without the need of modifying the actual arrangement of rebars to conform with the concrete FE mesh [12-13].

In order to optimize the performance of the Barzegar and Maddipudi [9] embedded mesh generation method, which is an extension of the work of Elwi and Hrudey [10], Markou and Papadrakakis [8] proposed the introduction of a geometrical constraint in order to decrease the computational effort for generating the input data of the embedded rebar elements, particularly when dealing with relatively large-scale numerical models. Their proposed method (Fig. 1) was incorporated in ReConAn FEA [5] which was developed and built to run in a 32-bit operating systems.

The purpose of this research work is to present the numerical performance of the embedded mesh generation method proposed by Markou [14] in the case of large-scale RC numerical simulations.

2 GENERATING REINFORCEMENT INSIDE HEXAHEDRAL ELEMENTS

The under study embedded mesh generation method considers arbitrary positioning of the rebars inside the concrete elements [8], as shown in Fig. 2, while avoiding a nonlinear search procedure for the calculation of the natural coordinates of the embedded reinforcement nodes in the corresponding prismatic hexahedral elements. By separating the mesh generation algorithm into to two main parts (Fig. 1), the geometry of each hexahedral element is categorized (prismatic or non-prismatic) and accordingly treated in order to compute the natural coordinates of its containing embedded rebar elements. For the detailed description of this method, refer to the relative reference [8].

The embedded reinforcement mesh generation method proposed in [8], was integrated and built in for a 64-bit operating system so as to overcome the problem that rises related to the physical memory allocation issue, which in the case of the 32-bit architecture is limited to 2 Gb. In addition to that the method was integrated with a filtering algorithm [14] that provides the ability to allocate relatively short embedded rebar finite elements, during the mesh allocation procedure. This filtering procedure provides the ability to control the mesh quality of the embedded rebar elements thus avoiding the numerical phenomenon of the local stiffness concentration due to the relatively short embedded rebar finite element length (Fig. 3). The flowchart diagram of the integrated embedded reinforcement mesh generation algorithm can be seen in Fig. 4.

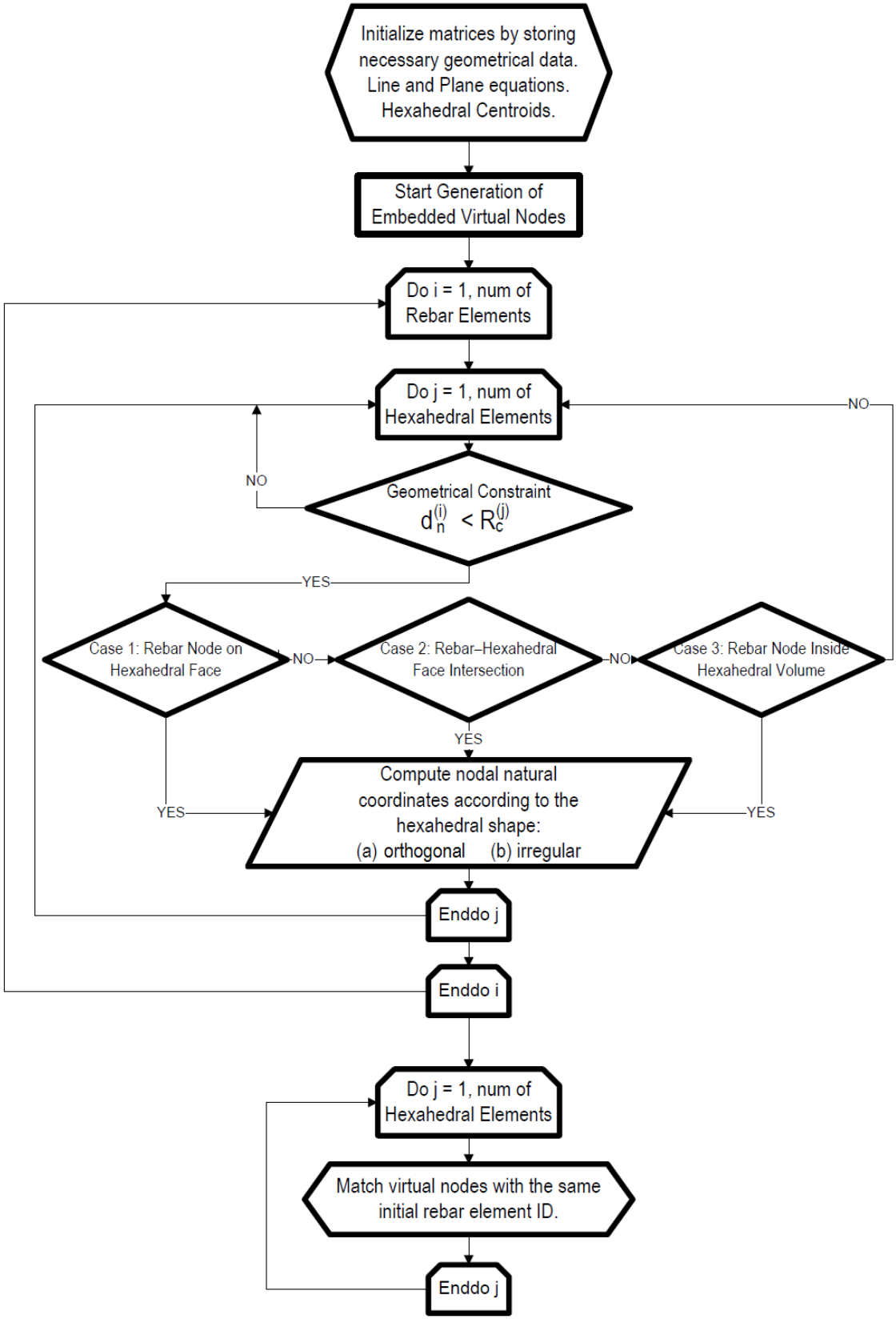

Figure 1. Flow chart of the embedded rebar mesh generation method [14].

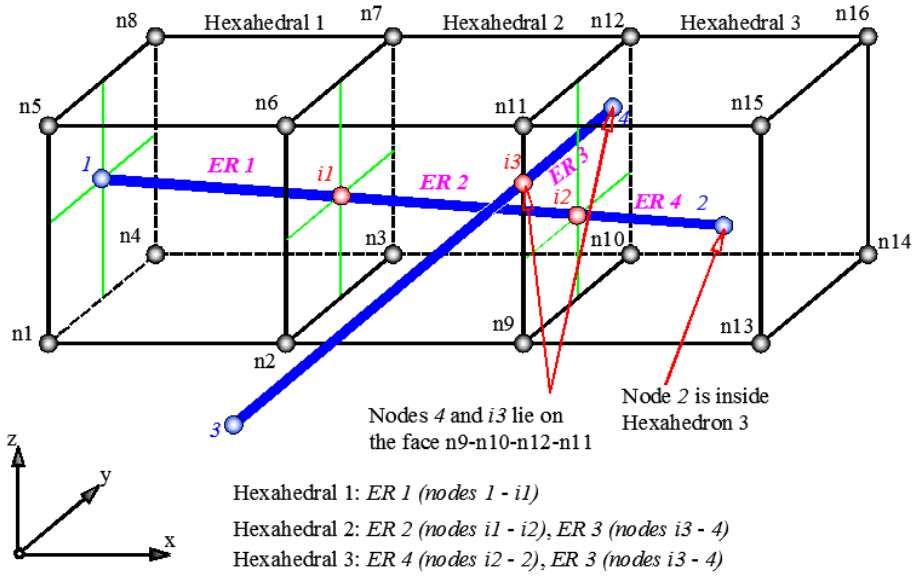

Figure 2. Embedded reinforcement rebars inside hexahedral elements [8].

As it can be seen in Fig. 4, the updated algorithm foresees the scanning of the rebar mesh so as to allocate short embedded elements that might result due to the irregular hexahedral mesh during the embedded rebar allocation procedure. In this case the embedded rebar mesh generation algorithm has the ability to filter the embedded rebar elements that have a very short length (see Fig. 3), while it controls the quality of the derived embedded mesh.

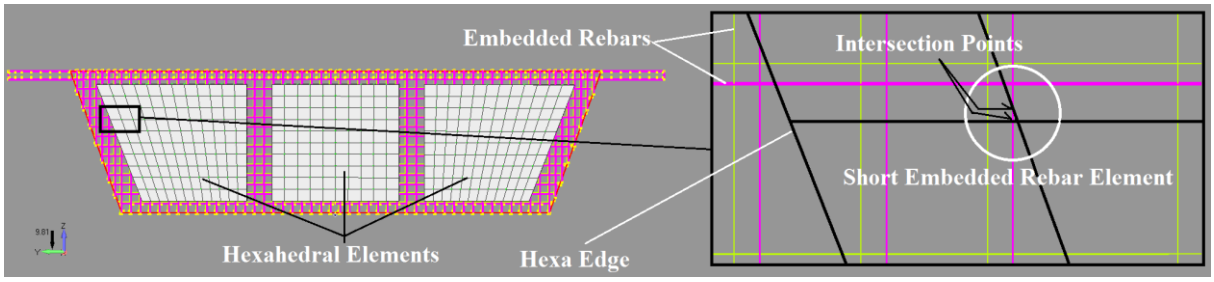

Figure 3. Hexahedral and embedded rebar elements of a RC bridge's vertical diaphragm. Short embedded rebar element case.

3 NUMERICAL IMPLEMENTATION

In order to assess the embedded mesh generation method, the Alhosn University's Male Campus and a RC bridge are used for constructing two 3D detailed meshes. The results from the embedded mesh generation procedures are discussed and the numerical results that derived from the solutions of the two models will be shortly presented. It must be noted that all numerical tests were performed on a 64-bit windows operating system (3.3GHz CPU).

3.1 RC Building

The RC building (Alhosn University Male Campus) that was used so as to construct the 3D mesh is shown in Fig. 5, while the geometry of its RC frame is given in Fig. 6. As it can be seen, the building has a total width of 20.45m and a 25.6m length. The total height of the building is 13.2m (Ground floor, 1st-3rd floor), while the basement of the structure is also accounted for in the under study model (Fig. 7).

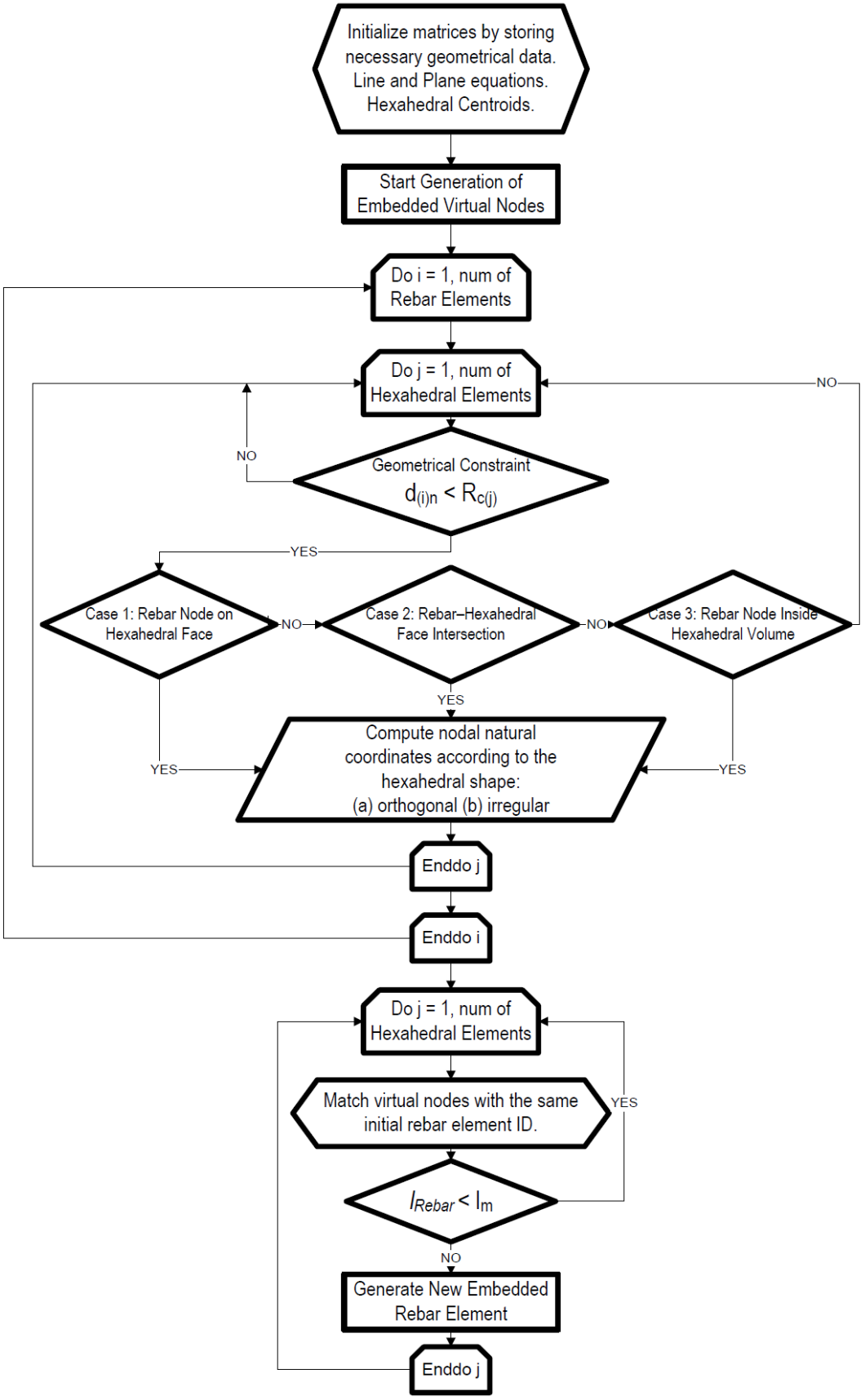

Figure 4. Flow chart of the updated embedded rebar element mesh generation method [14].

Figure 5. Alhosn University's Male Campus in Abu Dhabi, UAE.

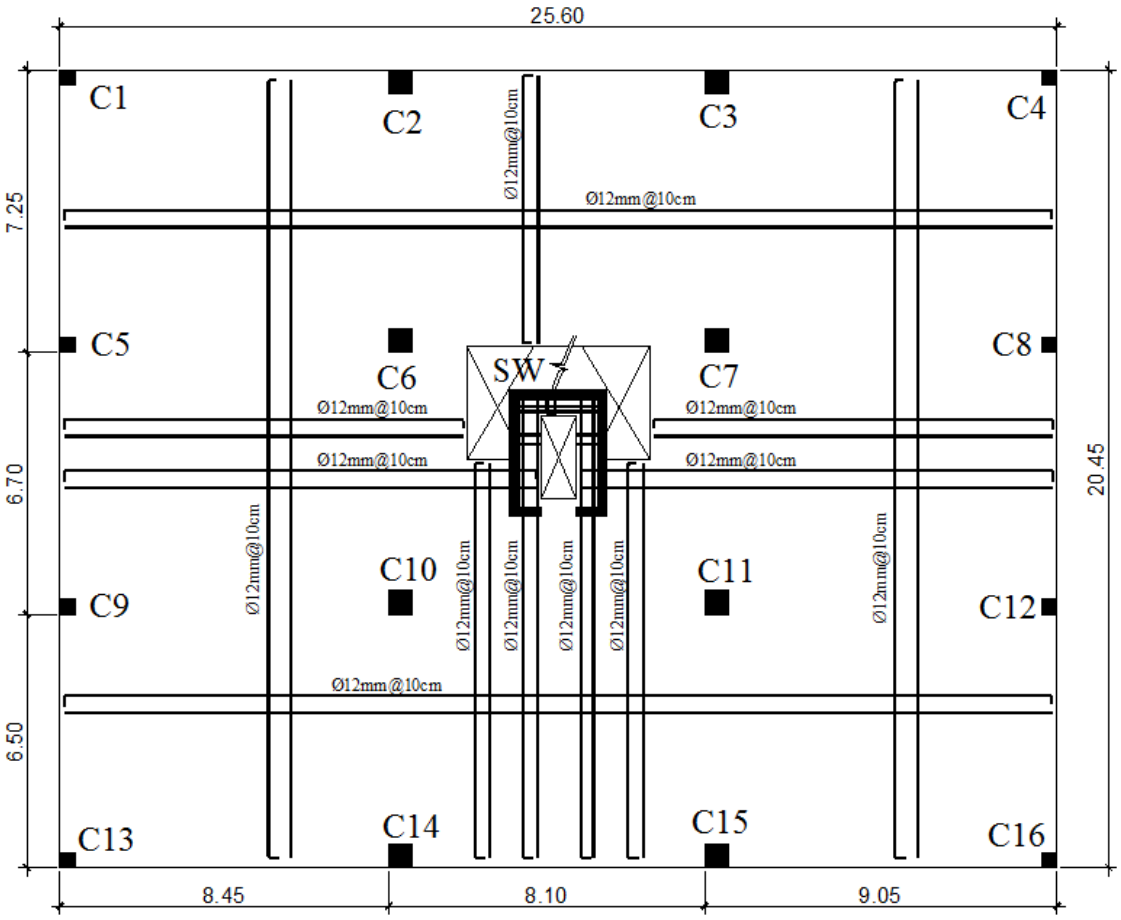

Figure 6. Reinforcement details of the slab (Ground – 3rd Floor).

In the UAE, the most common framing system used is that of the flat slabs, which is also the framing system adopted in this research work. As it can be depicted in Fig. 6, the shear wall of the elevator is located in the center of the structure, while a total of 16 columns are placed symmetrically about the structure's core. The geometry of the columns' sections are 40x40cm and 60x60cm. The thickness of the slab is assumed to be equal to 30cm while the reinforcement details are shown in Figs. 6 & 8. The 40x40cm columns are reinforced with 8Ø20mm longitudinal rebars and two hoops Ø8mm@10cm as stirrups, while the 60x60cm columns are reinforced with 12Ø22mm longitudinal rebars and three hoops Ø10mm@10cm

as stirrups. For the case of the shear wall, 72Ø18mm longitudinal rebars are used and Ø8mm@10cm as stirrups (Fig. 8).

Regarding the foundation type, it is assumed that the building is based on a general foundation slab which is 80cm thick. The foundation slab is reinforced with 14mm rebars every 10cm along the X and Y directions, while the foundation soil is also discretized with hexahedral elements in an attempt to make the numerical model more realistic. A retaining wall (Fig. 7) is foreseen at the perimeter of the basement which has a thickness of 20cm, which is reinforced with 12mm rebars at every 15cm as the principal reinforcement and 8mm rebars at every 15cm as the secondary reinforcement.

3.1.1. Construction and Management of the Hexahedral Mesh

ReConAn FEA uses Femap [15] through which the initial mesh is constructed, while the input file is exported into a text file (.neu → neutral file) that is used to generate the FE numerical model during the analysis of the numerical problem. For controlling the mesh quality the "Analysis by Parts" approach is used, which foresees the division of the mesh during the construction procedure into parts, while for each part an independent solution is performed to check for any mesh inconsistencies. Following the completion of this procedure all parts are combined and connected into the final mesh that is used to simulate the complete geometry of the structure. Fig. 9 shows the final mesh of the 75,080 8-noded hexahedral elements as it resulted from the mesh construction phase. The details related to the mesh are given in Table 1 and as it can be seen, the total number of concrete elements is 43,250, while the total number of nodes (excluding the embedded rebar macro-elements' nodes) is 119,232. The hexahedral edge size that was used to construct the concrete FE mesh of the RC frame was between 20-40 cm.

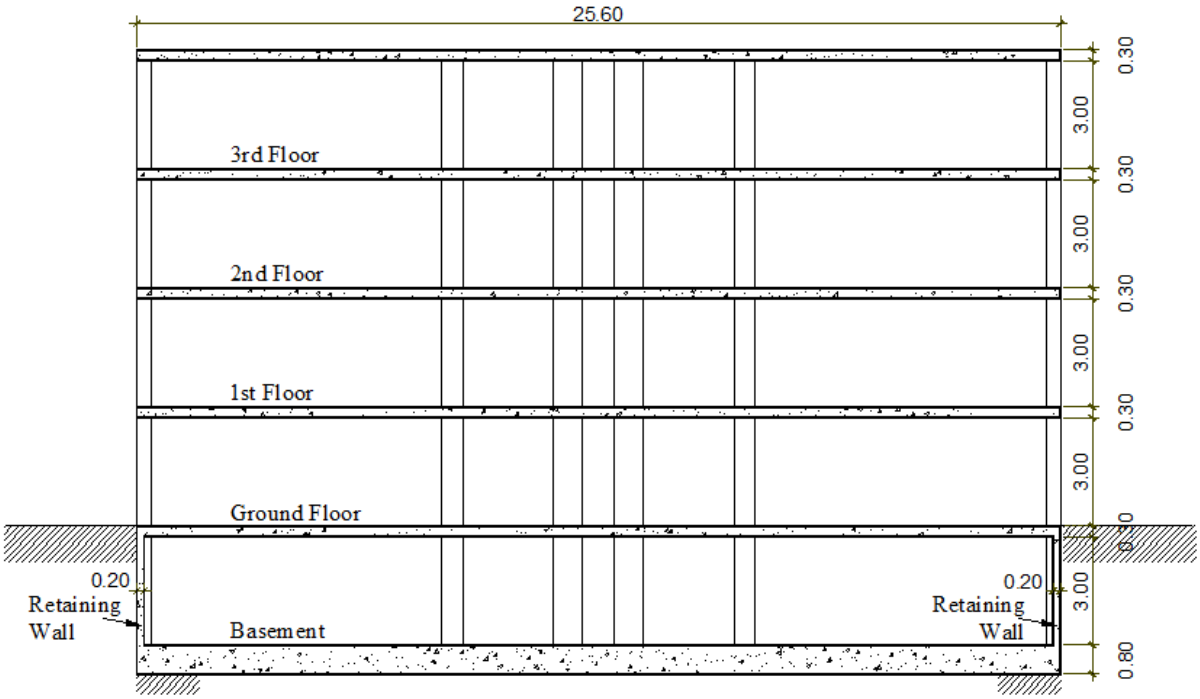

Figure 7. Section a-a of the building.

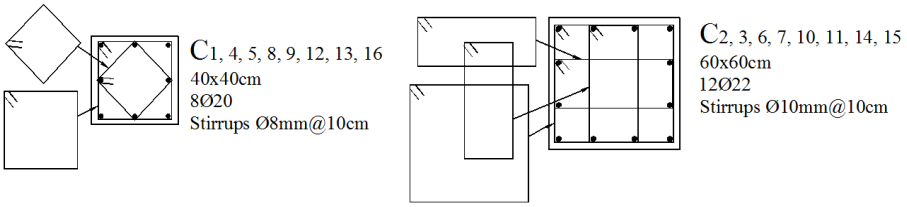

Note: Concrete cover 35 mm.

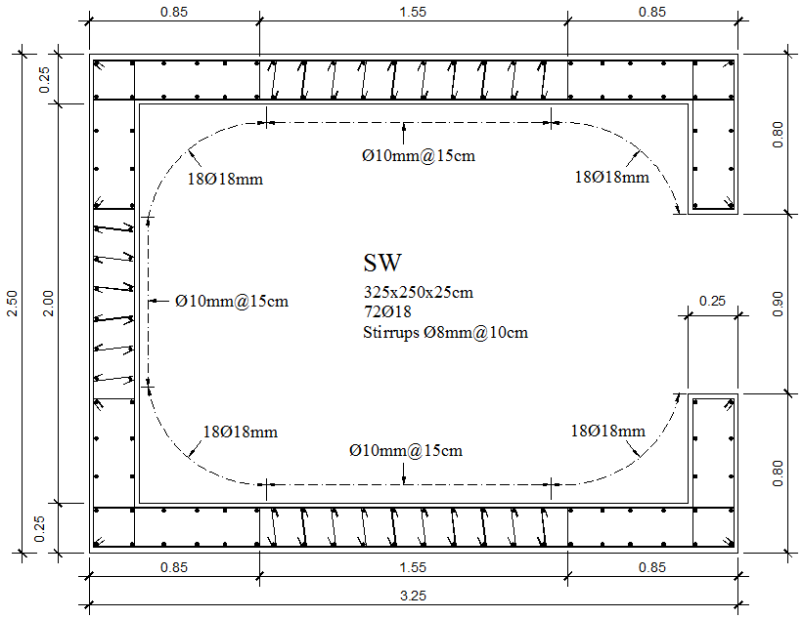

Figure 8. Reinforcement details of the columns and shear wall.

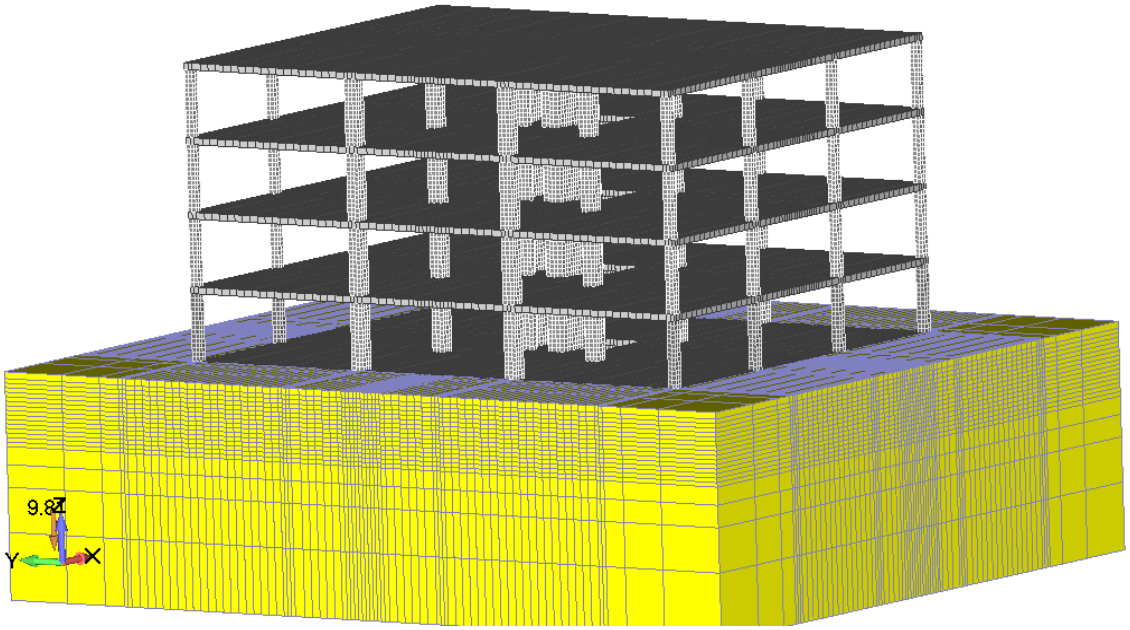

Figure 9. FE mesh of the 8-noded hexahedral elements.

The hexahedral mesh of the building was divided into 6 groups where each group was assigned with the corresponding Layers (a total of 25 layers). Fig. 10 shows the groups of Lay-

ers used during the hexahedral mesh construction procedure so as to manage graphically each part of the model. After the completion of the hexahedral mesh construction, the model was analyzed for the self-weight loads so as to ensure that the resulted numerical model was ready to be processed to the next stage which was the embedded rebar macro-element mesh construction. Fig. 11 shows the deformed shape and the von Mises stress distribution as it resulted from the Convergence Analysis stage (linear elastic analysis for the self-weight of the structure).

a/a	Description	Value
1	Hexa8 total number of Soil elements	31,830
2	Hexa8 Concrete elements	
	2.1 Foundation Slab	4,810
	2.2 Retaining Wall	3,630
	2.3 Slabs	23,410
	2.4 Columns 40x40	2,400
	2.5 Columns 60x60	5,400
	2.6 Shear Wall	3,600
	Total	43,250
3	Total number of Hexa8 elements	75,080
4	Total number of Hexa8 nodes	119,232

Table 1. FE mesh data related to the 8-noded hexahedral mesh.

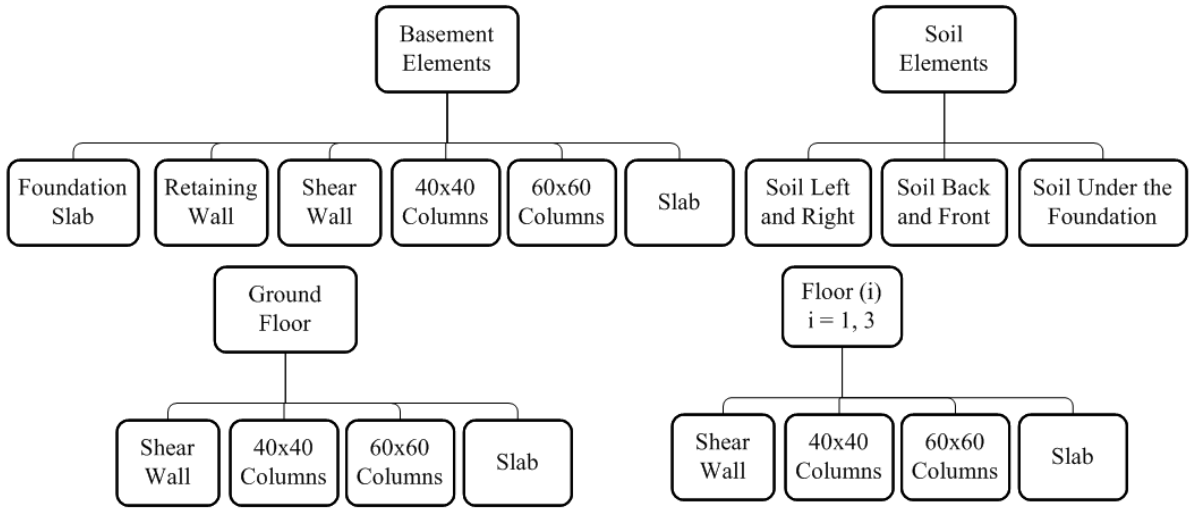

Figure 10. Layer organization chart of the hexahedral mesh.

3.1.2. Constructing, Managing and Verifying the Embedded Reinforcement FE Mesh

As it is shown in Fig. 12, the embedded rebar mesh was divided into 22 Layers according to the RC frame's geometrical features. Furthermore, after the completion of the construction of the embedded rebar macro-element mesh for each structural member of the basement's frame, a convergence analysis was performed (foundation slab, basement columns/shear wall/retaining wall/slab, see Figs. 13-14) so as to assess the derived FE mesh. After the successful completion of the convergence analysis, the embedded rebar macro-elements of the basement's frame were replicated to the rest of the floors deriving the final embedded rebar

macro-element mesh (see Table 2). Fig. 15 shows the final embedded reinforcement macro-elements as they resulted from the mesh construction procedure.

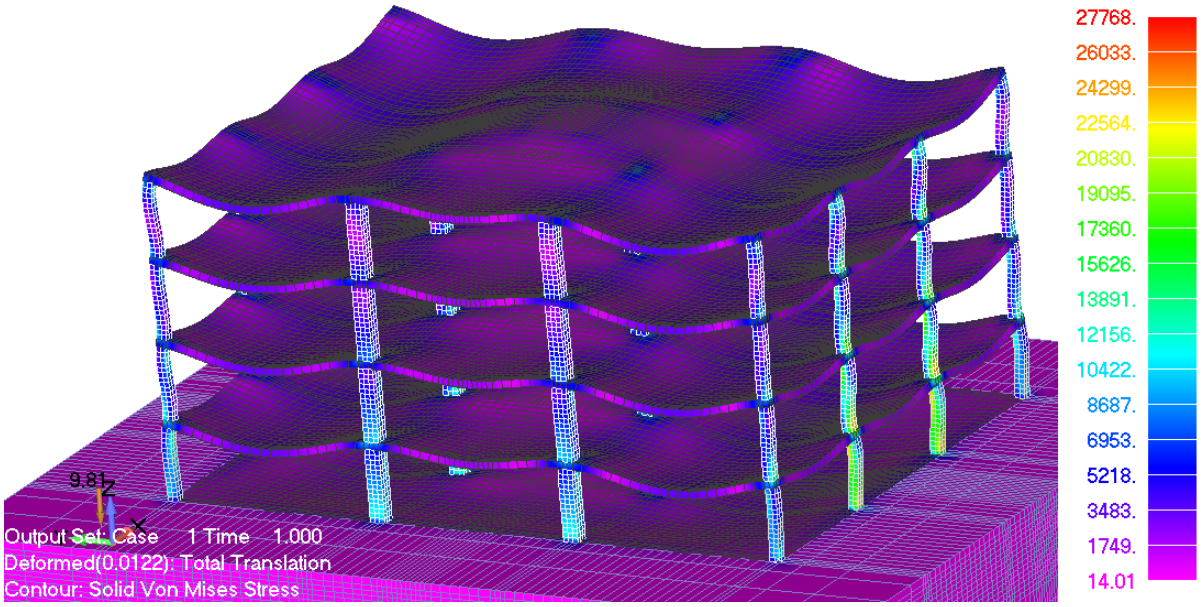

Figure 11. Deformed shape and von Mises stress distribution of the hexahedral mesh as it resulted from the Convergence Analysis stage.

a/a	Structural Member	*c*	Macro-Elements
1	Foundation Slab	20	9,712
2	Retaining Wall	3	14,304
3	Columns 40x40	3	13,824
4	Columns 60x60	3	20,736
5	Shear Wall	3	18,180
6	Slabs	20	53,503
		Total:	130,259
i	Basement with Foundation Slab	-	46,750
ii	Ground Floor		20,990
ii	1st Floor		20,990
iii	2nd Floor		20,990
iv	3rd Floor		20,539

Table 2. Embedded rebar macro-elements that derived from the mesh construction procedure.

3.1.3. Solution of the Complete Model

At this stage the complete model (Fig. 15) is going to be analyzed in order to allocate and generate the final embedded rebar mesh through the use of the under study embedded rebar mesh generation method. It must be noted at this point that the geometric constraint c [8] for the embedded rebar mesh generation procedure inside the vertical and horizontal structural members was set equal to 3 and 20, respectively, as it can be seen in Table 2. For the columns and shear walls the geometric constraint parameter c was set to 3 and for the rest of the frame equal to 20. Table 3 shows the details of the resulted FE mesh, the total required time for generating the embedded rebar elements and the numerical details related to the solution of the FE model.

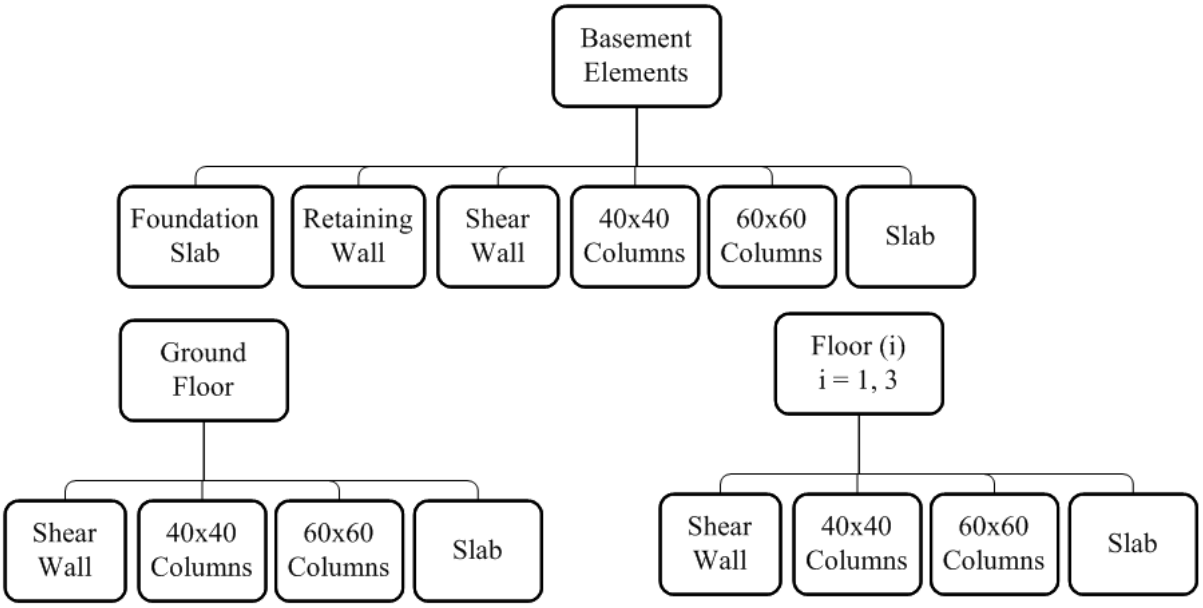

Figure 12. Layer organization chart of the embedded rebar macro-element mesh.

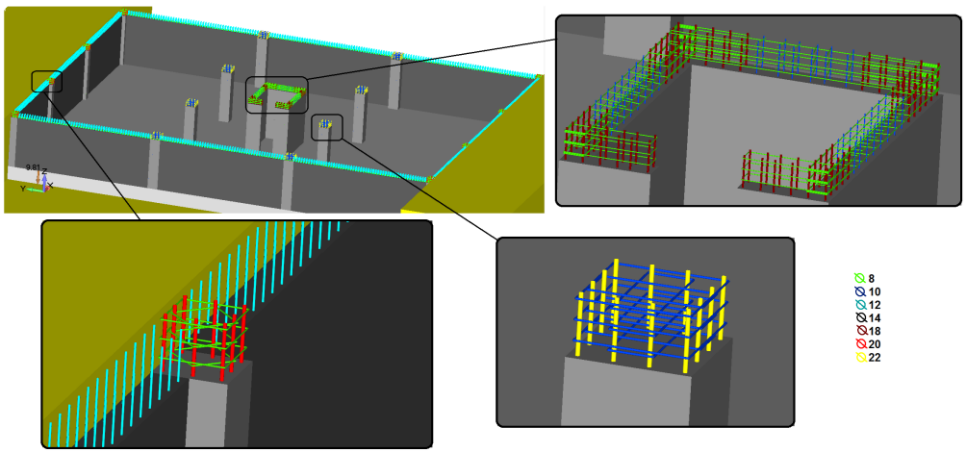

Figure 13. Macro-element rebar mesh construction phase. Hexahedral and macro-elements (Basement and Foundation Slab).

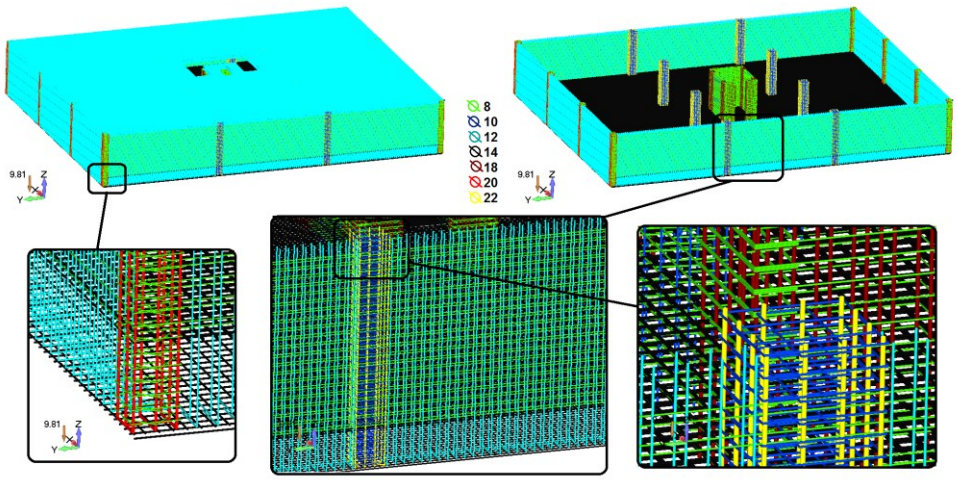

Figure 14. Macro-element rebar mesh of the Basement and the Foundation Slab (46,750 macro-elements).

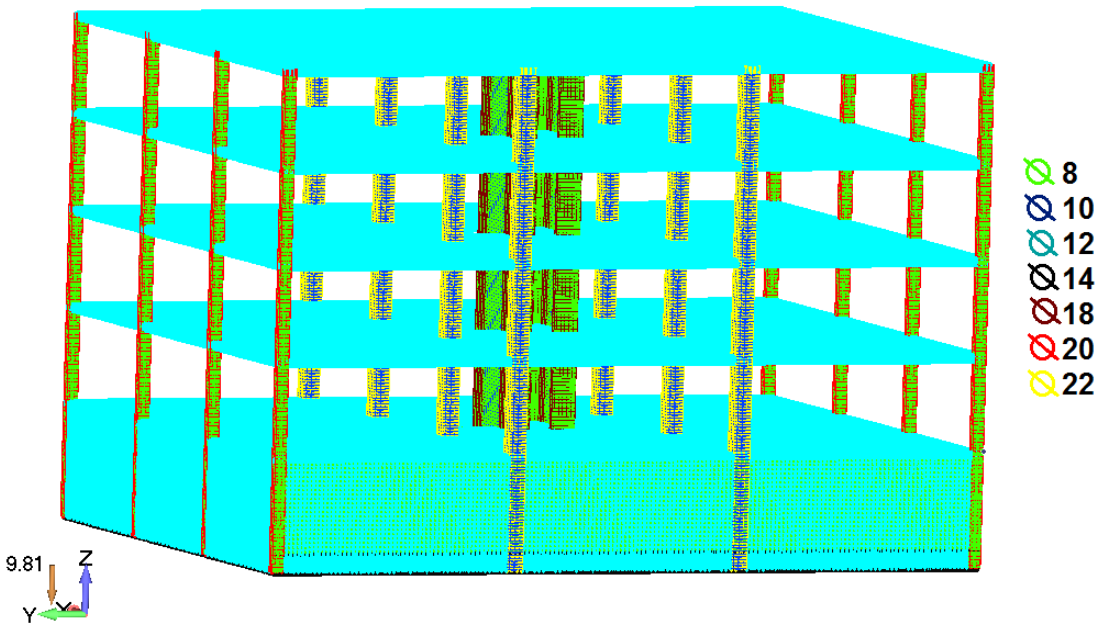

Figure 15. Macro-element rebar mesh of the RC frame of the building (130,259 macro-elements).

a/a	Description	Value
1	Number of Hexahedral Elements	75,080
2	Number of Nodes (hexa8 only)	119,232
3	Number of Macro-Elements	130,259
4	Total Number of Embedded Rebar FEs Generated	532,311
5	Total Number of Short Embedded Rebar FEs that were Discarded by the Filter Algorithm	5,408
6	Required Embedded Mesh Generation Time	75 min
7	Required RAM for the Stiffness Matrix	10.73 Gb
8	Number of Stiffness Matrix Elements	1,440,509,266
9	Total Required RAM for the Solution Procedure	22.73 Gb
10	Computational Time for Solving 1 Load Increment	52 min
11	Computational Time for Writing the Output Data	172 min
12	Total Computational Time: i. Read/Initialize Problem ii. Generate Embedded Mesh iii. Solve the System of Equations for 1 Load Increment / 1 Internal Iteration iv. Write Output Data (out.txt file size: 645 Mb) v. Other	324 min

Table 3. Numerical and computational results that derived after the solution of the complete FE model.

As it can be seen from Table 3, the total required time for the embedded mesh generation procedure was 75 minutes. The total number of generated embedded rebar FEs was 532,311 while the total number of short embedded rebar FEs that were discarded due to their small length was 5,408 (short length rebar criterion l_{min} = 5 mm). The deformed shape of the embedded rebar mesh resulted by applying only the self-weight of the structure (Figs. 16-17).

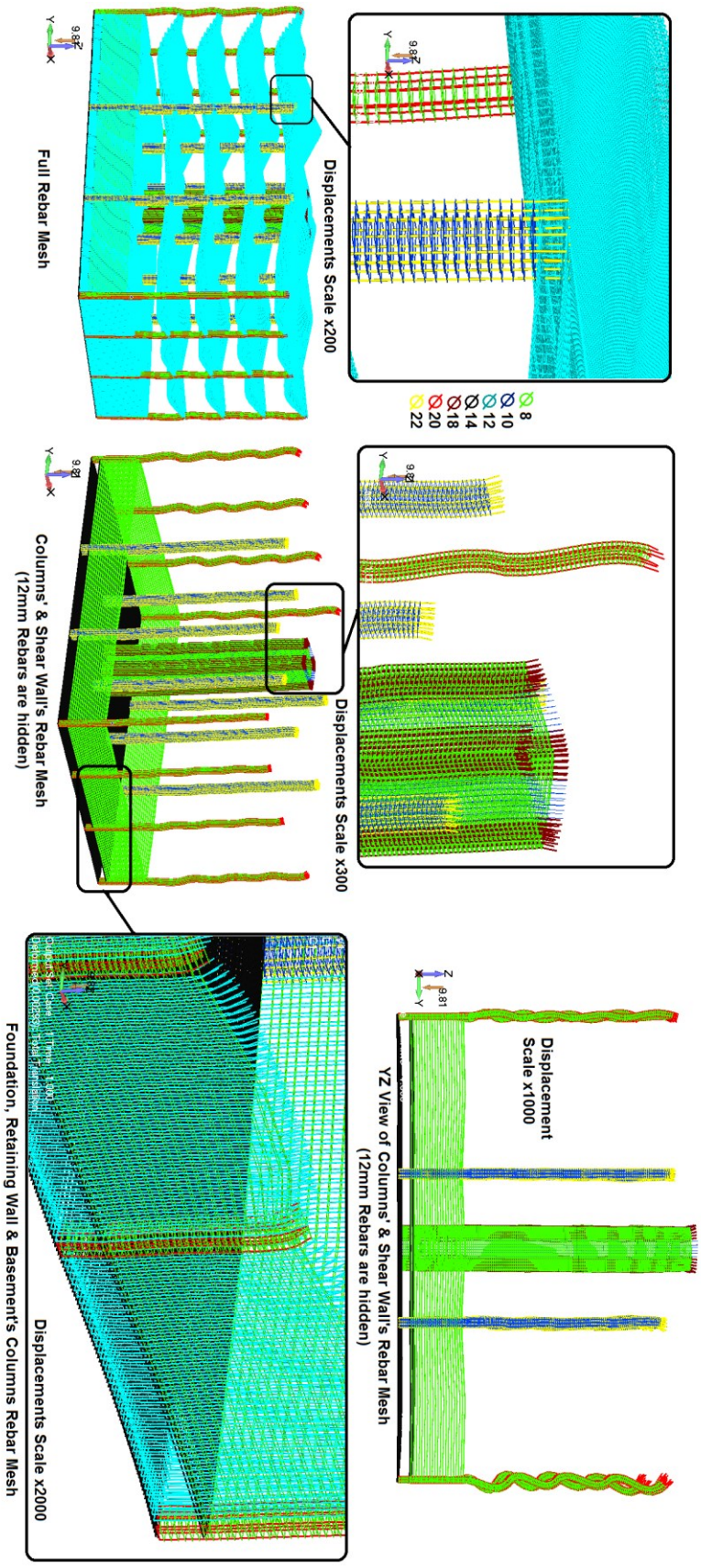

Figure 16. Deformed shape of the embedded rebar FE mesh.

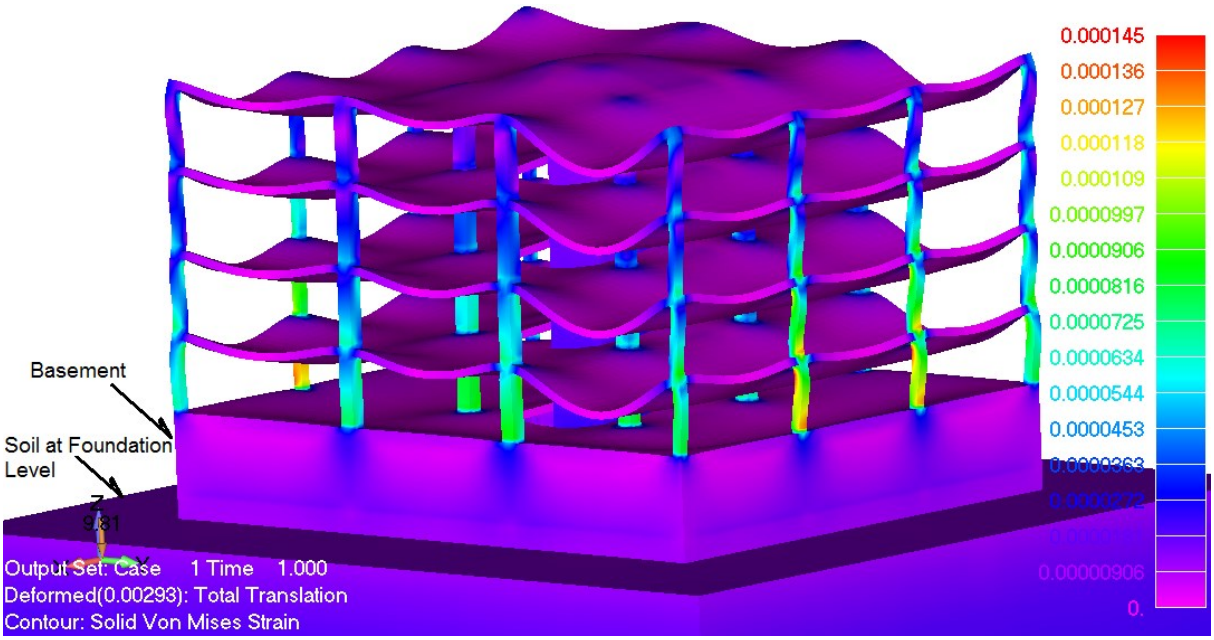

Figure 17. Deformed shape and von Mises strain distribution of the concrete elements.

In order to solve the numerical model for a single load increment, ReConAn required 52 minutes, while the total computational time was 324 minutes. The required embedded rebar mesh generation time represents 23.15% of the total computational time. The resulted computational ratio is relatively small given that the at hand numerical problem was solved for a single load increment, thus for the case of a nonlinear solution procedure with several load increments and internal iterations, the computational time of the actual nonlinear solution procedure would have been significantly larger. This is also verified through the next numerical implementation presented in this section. The requirements in RAM according to Table 3, shows that the allocation of the stiffness matrix requires the largest amount of physical memory than any other matrix used during the solution procedure. As it resulted the total required RAM for allocating the stiffness matrix for the at hand model was 10.73 Gb and to solve this numerical implementation a total of 22.73 Gb of RAM were required.

Fig. 16 shows the deformed shape of the embedded rebar mesh as it resulted from the analysis. The displacements are scaled so as to graphically represent the deformed shape of the frame (scale factors used in Fig. 16: x200-x2000). The deformed shape of the embedded rebar elements illustrate the robustness of the proposed embedded mesh generation method that manages to successfully allocate and generate more than half a million embedded rebar elements that are used to simulate the complete reinforcement grid of the under study RC structure. The deformed shape of the embedded rebar elements shows that their displacements, which are controlled by the hexahedral nodes' displacements, follow the concrete element mesh (Fig. 17) deformed shape. Fig. 17 shows the deformed shape and the von Mises strain distribution for the hexahedral elements as they resulted from the analysis procedure that was executed for the complete FE model. As it was expected, the superstructure undergoes a larger deformation in relation to the basement and the foundation soil that did not develop significant deformations (Fig. 17). Strain concentrations were mainly observed at the column-slab joints of the flat-slab framing system of the RC structure.

3.2 RC Arc-Shaped Bridge

This numerical test was chosen in order to illustrate the actual limitations of the embedded mesh generation method when dealing with large-scale implementations. The different stages until the solution of the full-scale model are described bellow.

3.2.1. Geometrical Features and Reinforcement Details of the RC Bridge

The geometry of the under study RC bridge is shown in Fig. 18. As it can be seen, the bridge has an effective span of 99.1 m, of which 51.55 m is the left span's length and 47.55 m is the right span's length. The total height of the two pylons is 5.1 m and the spacing between them is 5 m. A typical section of the bridge is given in Fig. 19, where the geometrical features can be depicted. The technical drawings show that the total width of the deck is 10.4 m and it has a height of 2.3 m. The different thicknesses of each structural component of the bridge's deck are given in Table. 4.

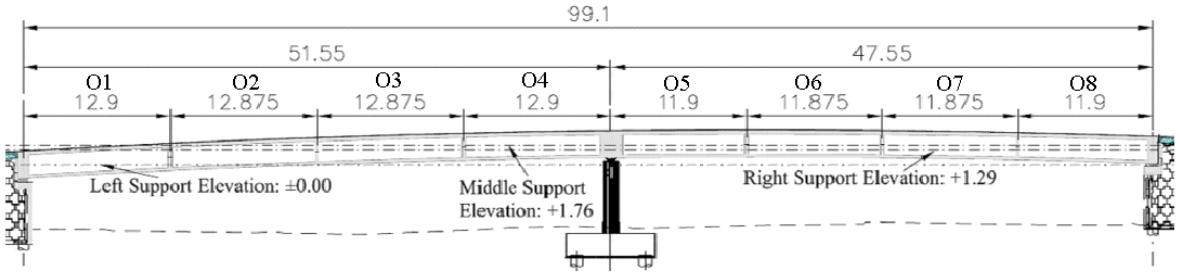

Figure 18. RC Bridge. View of elevations.

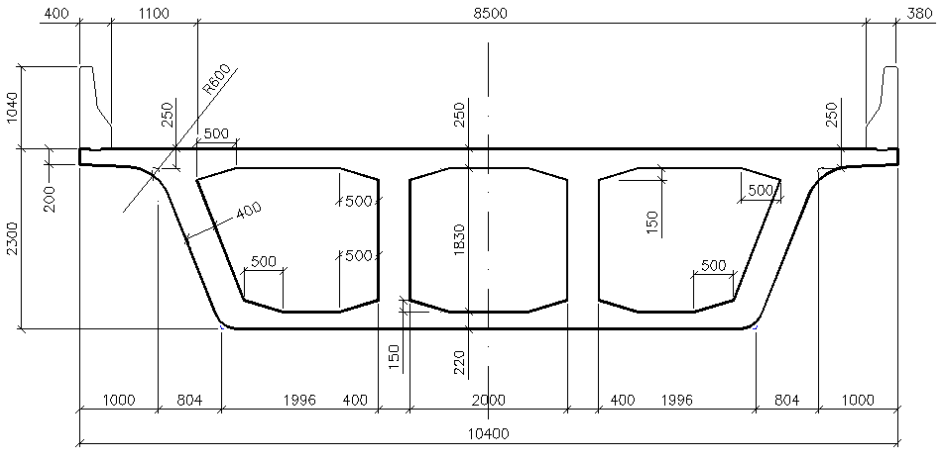

Figure 19. RC Bridge. Geometry of the section of the deck (dimensions in mm).

The reinforcement details of the Pylons are shown in Fig. 20, where it can be seen that 26 rebars of Ø32 mm are used and the stirrups have a diameter of Ø12 mm. Fig. 21 shows the reinforcement details of the pile cap. It is important to note that the model will assume fixed supports at the base of the pile cap, thus the 6 piles and the soil will not be included in the FE mesh.

Fig. 22 shows a typical deck section reinforcement detailing which foresees the use of 12, 16 and 20 mm rebars, while the geometry of the reinforcement arrangement of the support diaphragms can be depicted in Figs. 23 & 24.

a/a	Structural component	Thickness in cm
1	Upper Deck	25
2	Lower Deck	22
3	Overhangs	20
4	Vertical Walls	40
5	Vertical Diaphragms	30
6	Vertical Diaphragms at Supports	100
7	Vertical Diaphragm above Pylons	200

Table 4. RC Bridge. Thicknesses of different structural components of the deck.

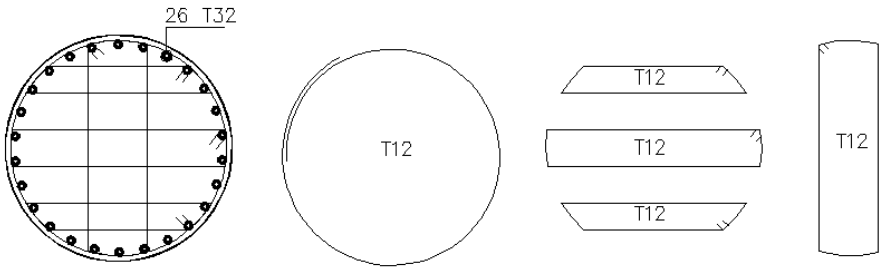

Figure 20. RC Bridge. Reinforcement details of the Pylon's section.

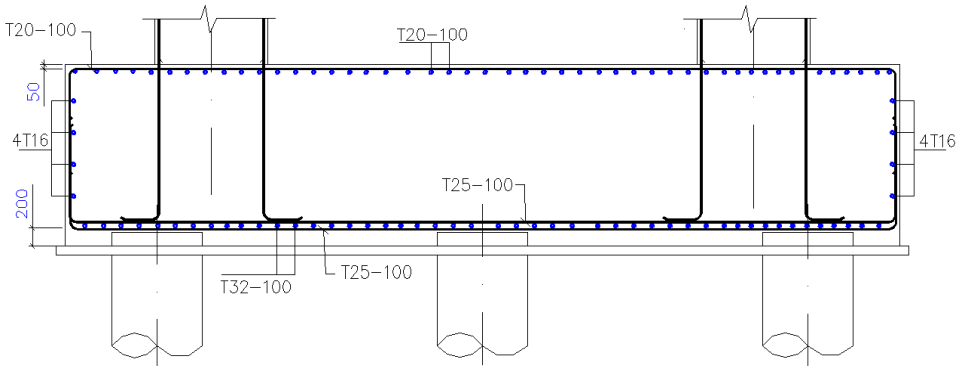

Figure 21. RC Bridge. Reinforcement details of the pile cap.

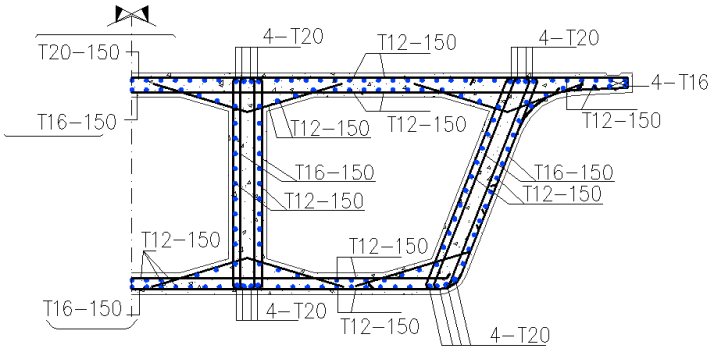

Figure 22. RC Bridge. Reinforcement details of a typical deck section.

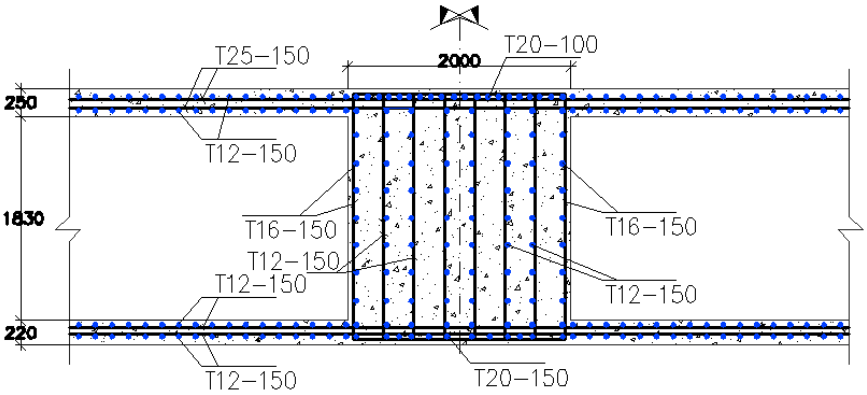

Figure 23. RC Bridge. Reinforcement details of the middle diaphragm.

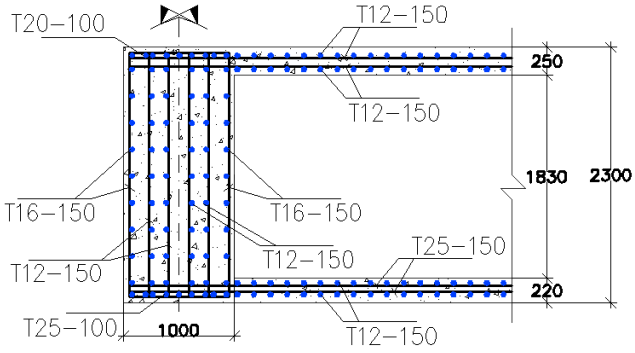

Figure 24. RC Bridge. Reinforcement details of the diaphragms at the left and right supports.

3.2.2. Constructing, Managing and Verifying the Hexahedral FE Mesh

Fig. 25 shows the final mesh of the 102,934 hexahedral elements (8-noded). The details related to the mesh are given in Table 5 and as it can be seen, the total number of concrete elements is 102,622, while the total number of nodes (excluding the embedded rebar macro-elements) is 168,400. The average hexahedral edge size used to derive the FE mesh of the RC bridge was 20 cm.

a/a	Structural Member	Hexa8
1	Opening O1 Deck + Left Support Diaphragm	13,824
2	Opening O2 Deck	11,254
3	Opening O3 Deck	11,254
4	Opening O4 Deck + Half of the Middle Diaphragm	12,662
5	Opening O5 Deck + Half of the Middle Diaphragm	12,432
6	Opening O6 Deck	10,558
7	Opening O7 Deck	10,558
8	Opening O8 Deck + Right Support Diaphragm	11,800
9	Two Pylons	3,080
10	Pile Cap	5,200
11	Elastomeric Bearings + Steel Plates	312
	Total	102,934

Table 5. RC Bridge. Hexahedral element distribution.

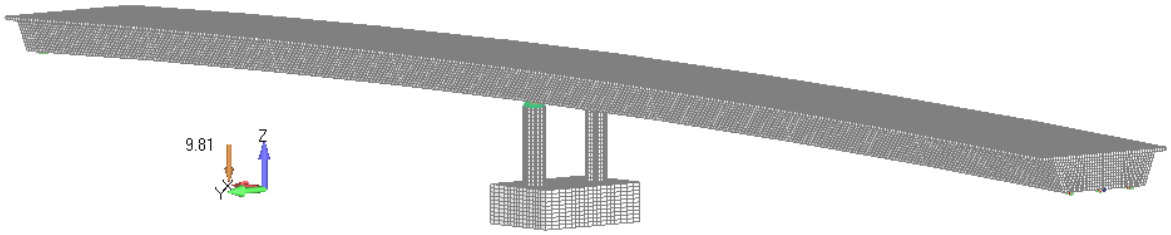

Figure 25. RC Bridge. FE mesh of 8-noded hexahedral elements.

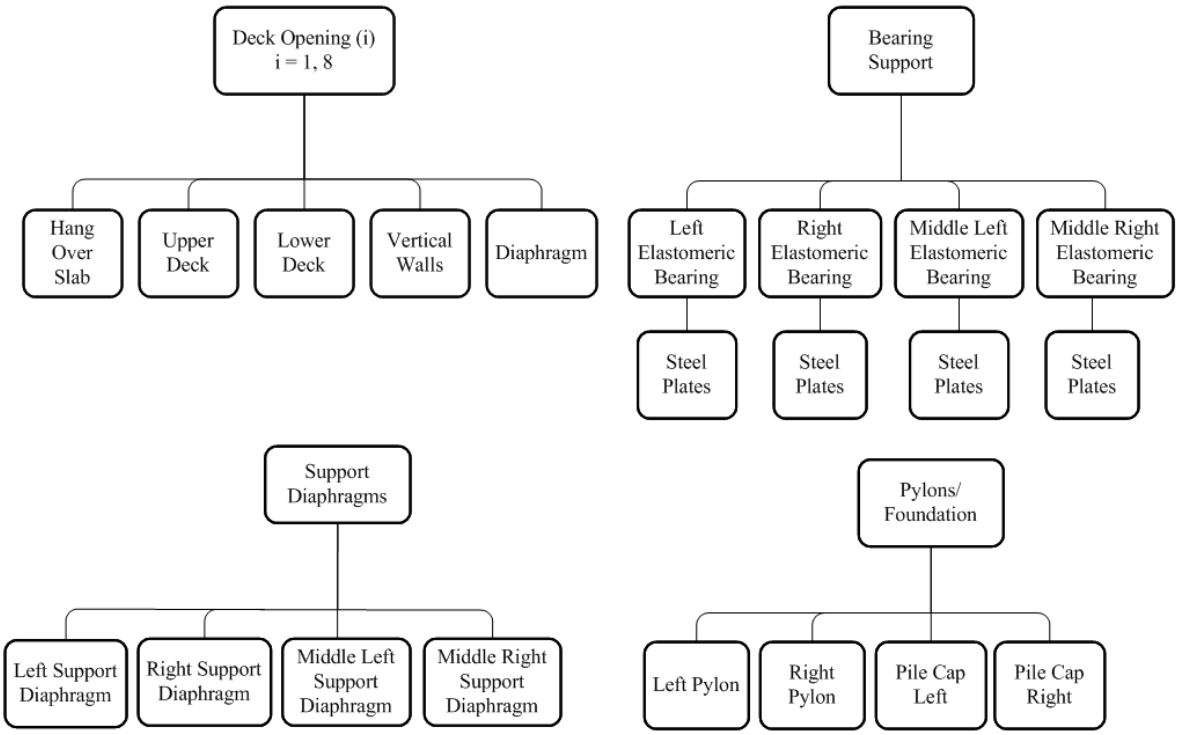

Figure 26. RC Bridge. Hexahedral mesh Layer organization chart.

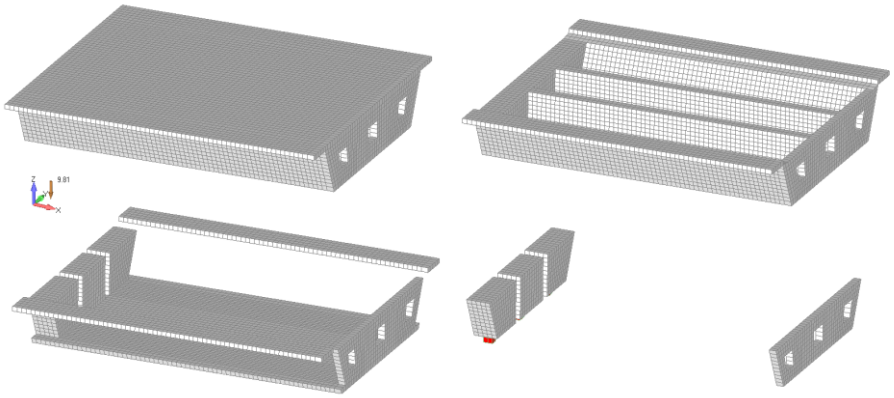

Figure 27. RC Bridge. Hexahedral mesh of the 1st Deck Opening O1. Graphical activation and deactivation of Layers.

The proposed logic behind the topological sorting of the Layers (Fig. 26) is based on the assumption that the hexahedral mesh of the bridge will be divided into four main groups of Layers (a. Deck Span, b. Bearing Supports, c. Support Diaphragms and d. Pylons/foundation), while in each main group of Layers the mesh of all structural members (Upper Deck, Vertical

Walls, etc.), which belong to a specific opening of the bridge, will be assigned into the designated Layer. The graphical illustration of the 56 Layers used in order to manage the hexahedral elements' mesh is shown in Fig. 26 and the use of Layers is demonstrated in Fig. 27 for the case of the deck opening O1.

The distribution of the hexahedral elements, according to the assumed Layers for the management of the hexahedral elements' mesh, are given in Table 5. It is evident that the largest number of hexahedral elements is located at the deck of the RC bridge. After the completion of the mesh convergence investigation, the resulted FE mesh consisted of 102,934 from which 102,622 are concrete hexahedral elements. The "Analysis by Parts" method was also implemented in order to verify that each part of the under construction hexahedral FE mesh (Fig. 28) was consistent, thus avoiding inducing numerical instabilities during the embedded mesh generation procedure and the analysis procedure of the complete model.

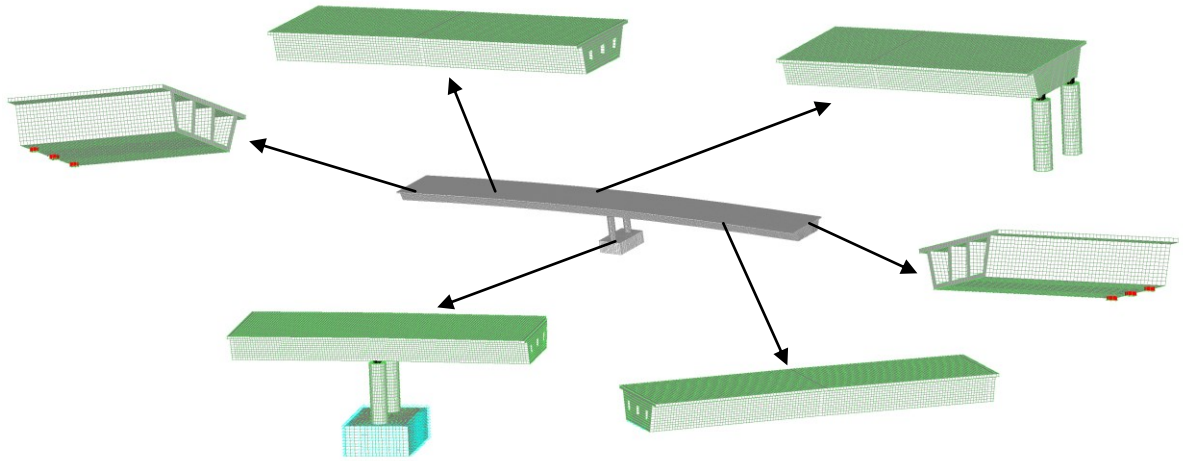

Figure 28. RC Bridge. Models used for the mesh convergence analysis procedure ("Convergence Analysis by Parts").

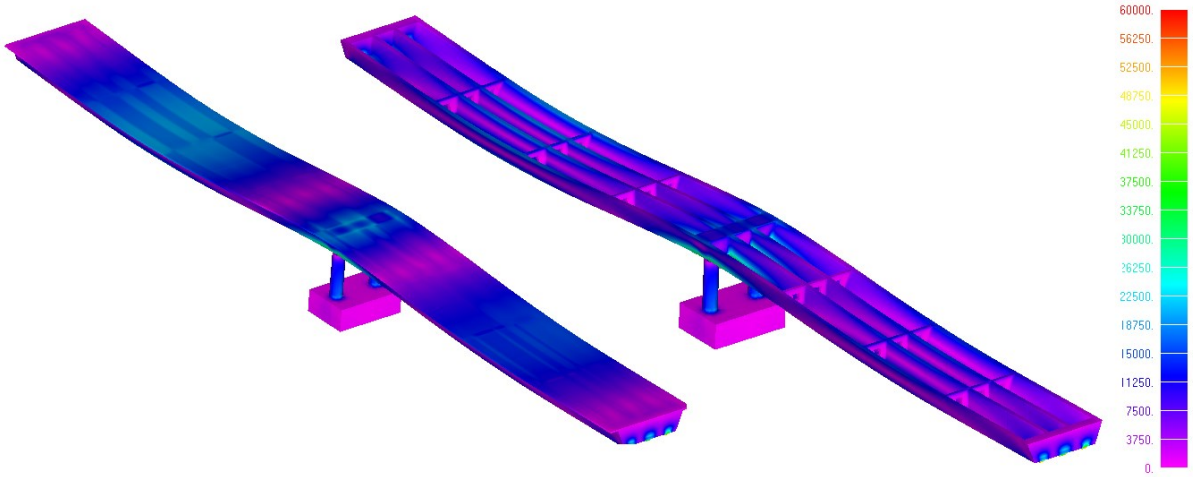

Figure 29. RC Bridge. Deformed shape and von Mises Stress contour. (Left) View of the full model and (Right) Internal view of the vertical and diaphragmatic walls.

The hexahedral mesh construction was finalized by performing the analysis of the complete hexa8 FE mesh by applying the self-weight of the structure. The deformed shape and the von Mises Stress distribution as they derived from the analysis are shown in Fig. 29. It must be noted here that the total number of unknowns for the case of the final hexahedral FE mesh was 502,478, the total number of the stiffness matrix elements was 657,655,263 and the re-

quired physical memory for solving the numerical model without the embedded reinforcement was 7.6 Gb.

3.2.3. Constructing, Managing and Verifying the Embedded Reinforcement FE Mesh

Given the fact that the required computational time for the analysis of this model will be significant, any mesh irregularities will induce numerical instabilities forcing the nonlinear analysis to terminate, while the size of the mesh will make it time-consuming if any mesh modification issues arise. For this reason the same mesh managing approach illustrated in the previous section was adopted in order to control the resulted embedded rebar mesh in a step-by-step logic (Layers and Analysis by Parts).

As it is shown in Fig. 30, the embedded rebar mesh was divided into 48 Layers according to the RC bridge's geometry. The 48 Layers were divided into 3 main groups so as to optimize the viewing procedure and the allocation of each reinforcement arrangement according to its positioning inside the structure. Furthermore, after the completion of the construction of the embedded rebar macro-element mesh for each structural member (see Table 6) of the bridge, a convergence analysis was performed so as to assess the derived FE model for each structural part of the bridge's model.

The embedded rebar mesh construction began by constructing and testing the Pylon/Pile Cap mesh (Fig. 31). The geometry of the hexahedral mesh of these structural members is irregular and mainly non-prismatic due to the circular sections of the pylons, while the embedded rebar mesh construction of the embedded rebar macro-elements was performed by using long macro-elements that intersect more than 15 hexahedral elements. In some areas of the Pile Cap mesh, rebar macro-elements penetrate up to 20 hexahedral elements.

a/a	Structural Member	*c*	Macro-Elements	Embedded Rebar FEs
1	Span O1 Deck + Left Support Diaphragm (Fig. 41)	15	6,721	70,614
2	Span O2 Deck (Fig. 42)	15	5,092	61,476
3	Span O3 Deck (Fig. 43)	15	5,100	62,954
4	Span O4 Deck (Fig. 44)	15	4,046	50,401
5	Middle Diaphragm (Fig. 45)	30	1,656	25,172
6	Span O5 Deck (Fig. 46)	15	4,601	52,673
7	Span O6 Deck (Fig. 47)	15	4,805	56,416
8	Span O7 Deck (Fig. 48)	15	4,818	55,693
9	Span O8 Deck + Right Support Diaphragm (Fig. 49)	15	5,546	63,504
10	Two Pylons and Pile Cap (Figs. 38 & 39)	5 | 15	5,454	21,721
		Total	47,839	520,624

Table 6. RC Bridge. Embedded rebar macro-elements and resulted embedded rebar FEs that derived from the procedure of the convergence analysis by parts.

After the completion of the embedded rebar macro-element mesh of the Pylons and the Pile Cap, the model was analyzed in order to assess the resulted FE mesh. During the embedded mesh generation procedure, for the case of the Pile Cap, the incremental parameter c was set equal to 15 and for the case of the Pylons, equal to 5. The total number of the embedded rebar elements that were generated was 21,721.

Fig. 32 shows the deformed shape of the embedded rebar mesh as it derived from the analysis of the model. As it can be seen, the mesh generation procedure managed to allocate the embedded rebar elements without any numerical instabilities, while the irregular geometry of

the hexahedral elements did not result any numerical issues during the mesh generation procedure. The deformed shape and stress contour shown in Fig. 32 resulted by applying the self-weight of the structure and a distributed load of 1 kN/node at the tip of each Pylon.

Table 6 shows the distribution of the total number of the embedded rebar macro-elements used to construct the reinforcement grid of the RC bridge. As it can be depicted, the total number of embedded rebar macro-elements used was 47,839 and the total number of embedded rebars that were generated through the Analysis by Parts procedure was 520,624. It must be noted here that the parameter c was set between 5-30 (Table 6) given that the macro-elements were constructed so as to penetrate between 1-30 hexahedral elements.

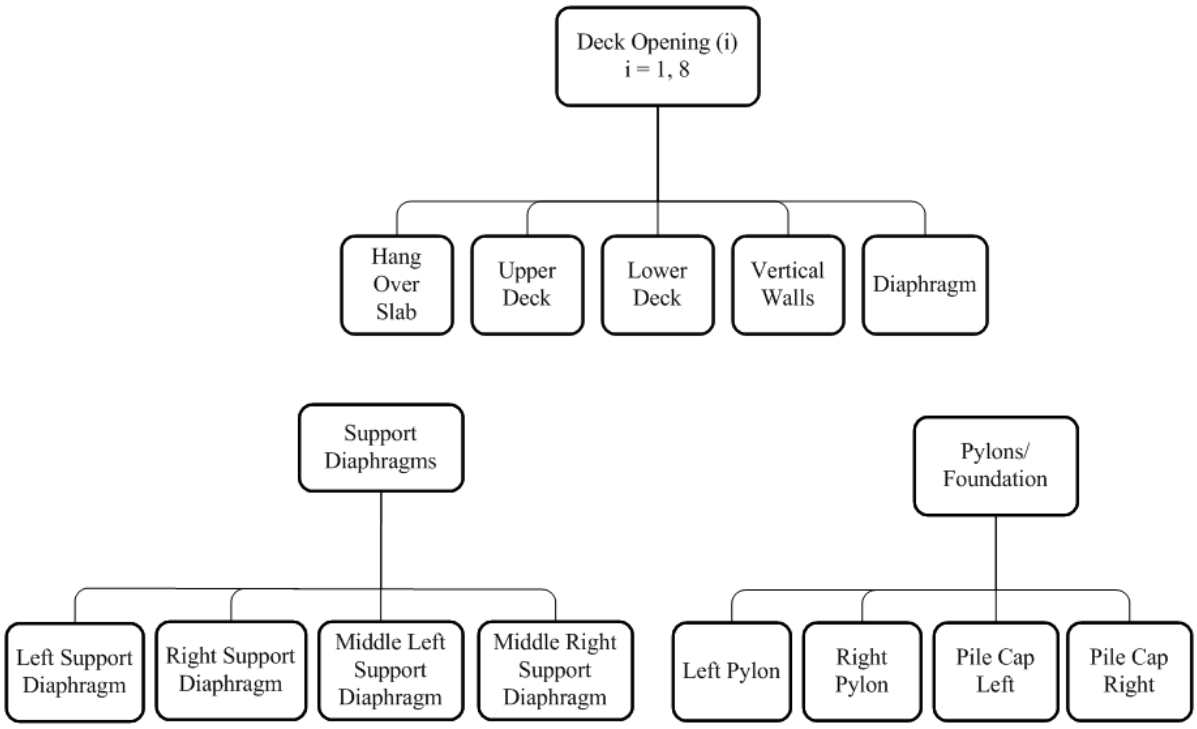

Figure 30. RC Bridge. Embedded rebar mesh Layer organization chart.

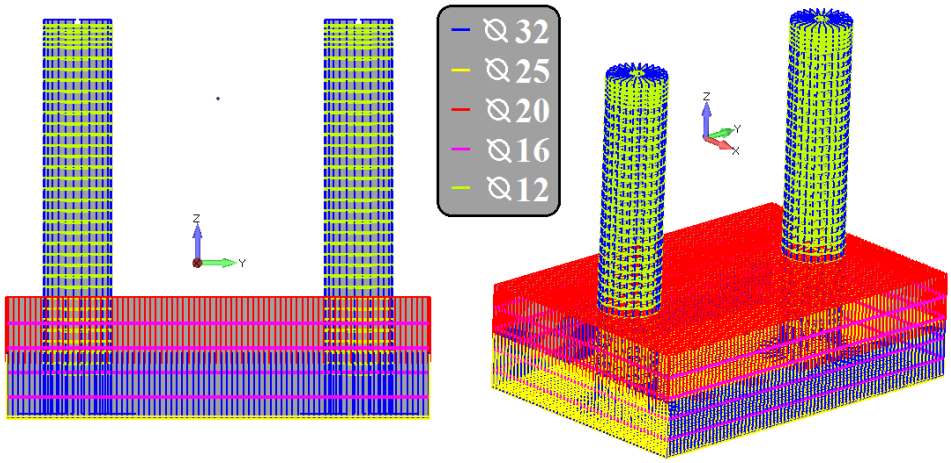

Figure 31. RC Bridge. Embedded rebar mesh of the Pylons and Pile Cap (5,454 embedded rebar macro-elements).

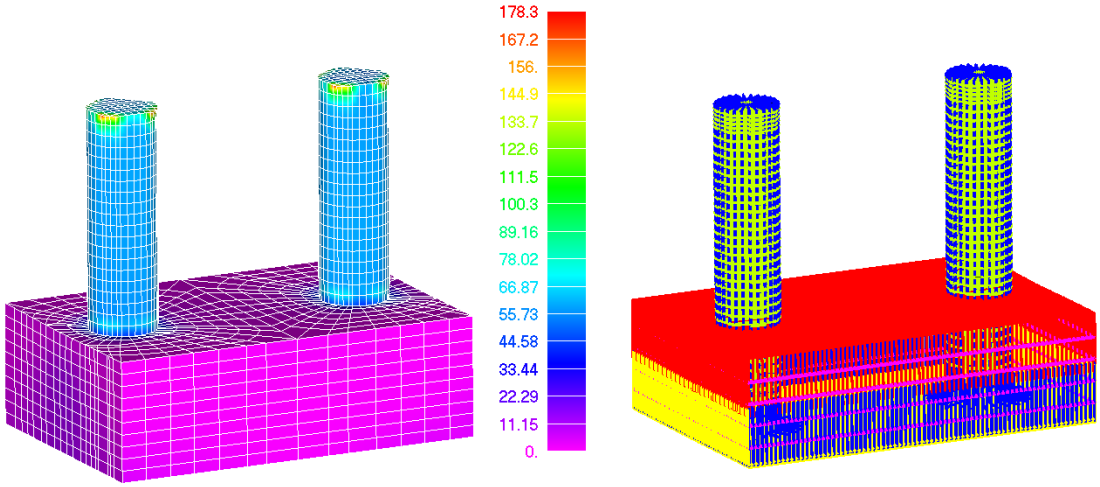

Figure 32. RC Bridge. (Left) von Mises Stress contour and (Right) Deformed shape of the embedded rebar elements of the two Pylons and the Pile Cap (21,721 embedded rebar elements generated).

3.2.4. Solution of the Complete Model

At this stage the complete model (Fig. 33) can be used so as to allocate and generate the final embedded rebar mesh through the use of the integrated embedded mesh generation method. Table 7 shows the details of the resulted FE mesh, the total required time for generating the embedded rebar elements and numerical details related to the solution of the FE model.

a/a	Description	Value
1	Number of Hexahedral Elements	102,934
2	Number of Nodes (hexa8 only)	168,400
3	Number of Macro-Elements	47,839
4	Total Number of Embedded Rebar FEs Generated	520,624
5	Total Number of Short Embedded Rebar FEs that were Discarded by the Filter Algorithm	1,439
6	Required Embedded Mesh Generation Time	42 m 22 s
7	Required RAM for the Embedded Mesh Generation	2 Gb
8	Required RAM for the Stiffness Matrix	5.225 Gb
9	Max Required RAM Allocated by the Software	11.5 Gb
10	Computational Time for Solving 1 Load Increment	18 m
11	Computational Time for Writing the Output Data	53 m
12	Total Computational Time: i. Read/Initialize Problem ii. Generate Embedded Mesh iii. Solve the System of Equations for 1 Load Increment / 1 Internal Iteration iv. Write Output Data (out.txt file size: 475 Mb)	118 m

Table 7. RC Bridge. General numerical details that derived after the solution of the complete FE model.

As it can be seen from Table 7, the total required time for the embedded mesh generation procedure was 42 minutes 22 seconds and the corresponding required RAM allocated for this task was 2 Gb. The total number of generated embedded rebar FEs was 520,624 while the total number of short embedded rebar FEs that were discarded due to their small length was 1,439. The deformed shape of the embedded rebar mesh (Fig. 34), resulted by applying only

the self-weight of the structure. The solution of the complete model required a total of 11.5 Gb of RAM from which the 5.225 Gb was required for the stiffness matrix allocation. So as to solve the model for a single load increment, ReConAn required 18 minutes, while the total computational time for reading, initializing, generating the embedded mesh, solving the system of equations (for 1 load step and 1 internal iteration) and writing the output data, was 118 minutes. The required embedded mesh generation time represents 36% of the total operation time. This ratio is relatively small given that the numerical problem foresees the solution of 1 load increment and 1 internal iteration. In addition to that, the numerical results illustrate the significance of having a computationally robust and efficient embedded mesh generation procedure.

As it can be seen in Fig. 34, the deformed shape of the embedded rebar mesh was graphically illustrated by increasing the derived displacements 500 times. The deformed shape shows that the embedded rebar mesh follows the sinusoidal deformed shape of the bridge's deck as it resulted from the numerical solution procedure.

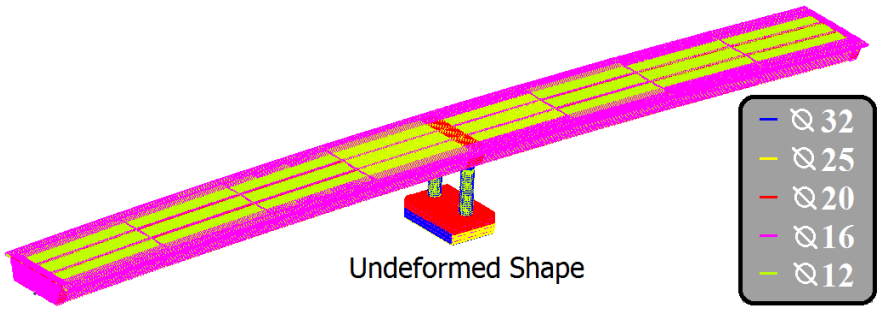

Figure 33. RC Bridge. Macro-element rebar mesh.

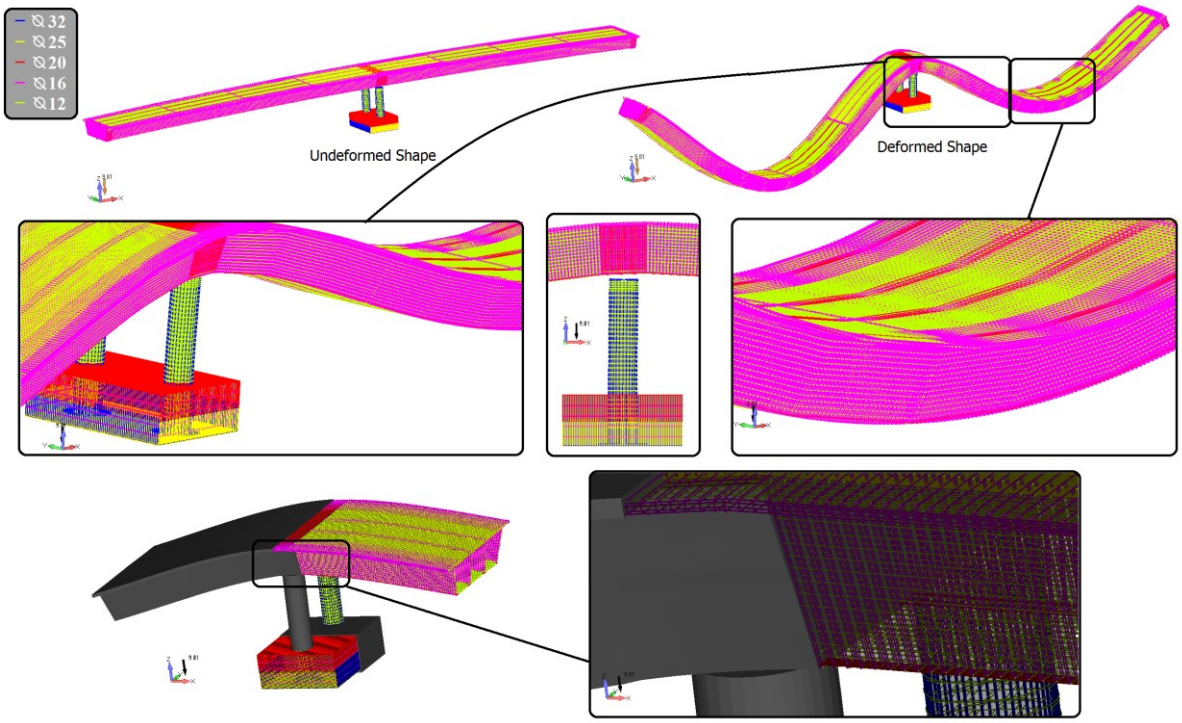

Figure 34. RC Bridge. Deformed shape of the embedded rebar FE mesh.

After applying a vertical nonlinear load of 135,125MN, which was distributed uniformly along the area of the deck, the numerical problem was solved and the resulted crack pattern

for 60% of the total applied load is shown in Fig. 35. The solution procedure failed to converge when 90% of the total nonlinear load was applied. For solving the 8 load increments the solver required 24 hours and to write the output data 8 hours. This means that the required embedded rebar mesh generation procedure requires less than 3% of the total computational time illustrating the numerical efficiency of the embedded rebar mesh generation method.

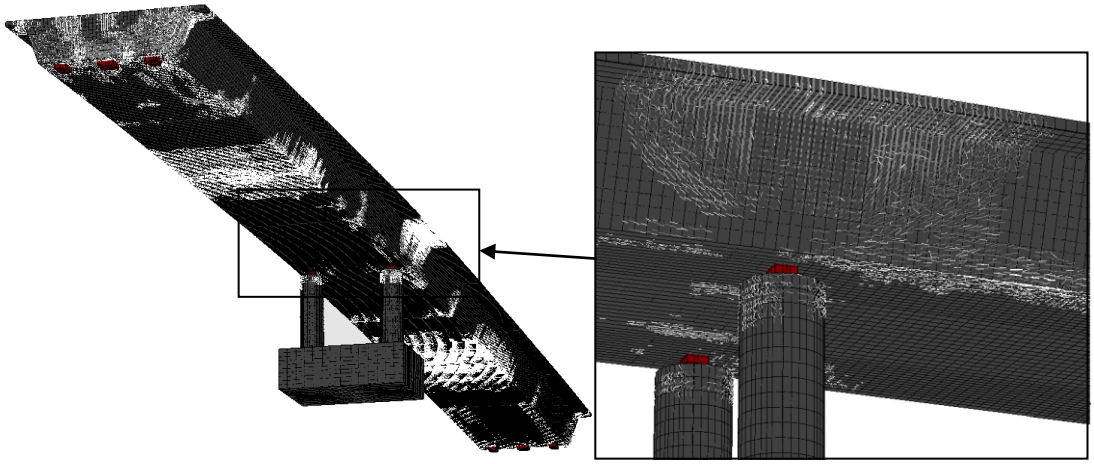

Figure 35. RC Bridge. Crack pattern for 60% of the total applied load.

3.2.5. Double Deck Model

In an attempt to increase the previous FE mesh so as to further investigate the numerical performance of the under study mesh generation method, the numerical model that was presented in Fig. 33 is increased by replicating the bridge one time. Fig. 36 shows the new mesh, while in Table 8 the numerical details related to the mesh can be depicted.

Table 8 shows the numerical details that derived after the solution of the increased mesh, where it can be seen that the total number of embedded rebar elements that were generated was 1,052,892. If the number of generated embedded rebar elements is compared with the one that resulted from the previous section, then it will result that an additional 11,644 embedded rebar elements were generated. This is attributed to the connection beam that connects the two pile caps as shown in Fig. 36. The embedded mesh generation procedure managed to complete the embedded rebar allocation/generation procedure in 304 minutes and 5 seconds.

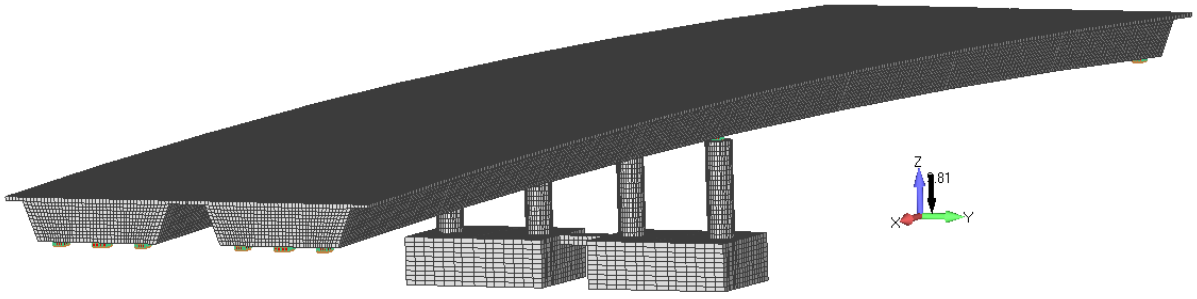

Figure 36. Double Deck RC Bridge. FE mesh of 8-noded hexahedral elements.

The required computational time for the embedded rebar mesh generation procedure represents the10.48% of the total computational time. An important observation that derives by comparing the new ratio with that resulted in the previous section (36%), is that the computational performance of the under study method maintained its efficiency in relation to the solution algorithm that required an excessive time so as to solve a single load increment. This also

underlines the need of using a parallel solver that will significantly reduce the computational time for solving the system of equations.

Fig. 37 shows the deformed shape of the model as it resulted from the numerical analysis. As it can be seen, the embedded rebar elements have the same deformed shape thus follow the deformation of the concrete domain.

a/a	Description	Value
1	Number of Hexahedral Elements	205,928
2	Number of Nodes (hexa8 only)	336,908
3	Number of Macro-Elements	95,082
4	Total Number of Embedded Rebar FEs Generated	1,052,892
5	Total Number of Short Embedded Rebar FEs that were Discarded by the Filter Algorithm	2,878
6	Required Embedded Mesh Generation Time	304 m 5 s
7	Required RAM for the Stiffness Matrix	19.52 Gb
8	Max Required RAM Allocated by the Software	30.0 Gb
9	Computational Time for Solving 1 Load Increment	27 hr
10	Computational Time for Writing the Output Data	10 hr 32 min
11	Total Computational Time: i. Read/Initialize Problem ii. Generate Embedded Mesh iii. Solve the System of Equations for 1 Load Increment / 1 Internal Iteration iv. Write Output Data (out.txt file size: 970 Mb)	48 hr 29 min

Table 8. Double Deck RC Bridge. General numerical details that derived after the solution of the complete FE model.

4 CONCLUSIONS

The integrated embedded mesh generation method, which is an extension of the Markou and Papadrakakis method [8], was used to generate the embedded rebar mesh of a RC building and a RC bridge. The parametric investigation performed for the required computational time in generating the embedded rebar elements, in a 64-bit operating system, verifies the computational robustness and efficiency of the method in generating embedded rebar finite elements inside regular and irregular hexahedral meshes.

For the case of the RC building, the FE mesh that was used consisted of 75,080 hexahedral elements and 130,259 embedded rebar macro-elements. After performing the analysis for this numerical implementation it derived that the embedded rebar mesh generation method managed to allocate 537,719 embedded rebar elements from which 5,804 had a length shorter than 5 mm and were excluded from the analysis procedure. The mesh generation procedure required 75 minutes.

In order to further investigate the performance of the integrated embedded rebar mesh generation method, a full-scale model of a RC bridge was constructed and analyzed. The construction of the model eventually derived a total number of 102,934 hexahedral elements and 47,839 embedded rebar macro-elements. After mesh generation procedure, the derived RC bridge numerical model consisted of 623,576 finite elements from which 102,622 are hexahedral concrete FEs that treat the cracking phenomenon with the smeared crack approach. Solving a FE model that incorporated a numerically unstable material formulation with numerical

discontinuities is by default a cumbersome procedure even for benchmark problems that assume a limited number of hexahedral elements (100-1000 hexahedral elements). Dealing with a large-scale numerical simulation, controlling the resulted FE mesh from the embedded rebar mesh generation level is of significant importance given that it controls the numerical outcome of the embedded mesh generation and solution procedures. The mesh generation procedure required 42 minutes 22 seconds, which illustrates the computational efficiency of the method, while the limitations of the embedded mesh generation algorithm were not practically reached.

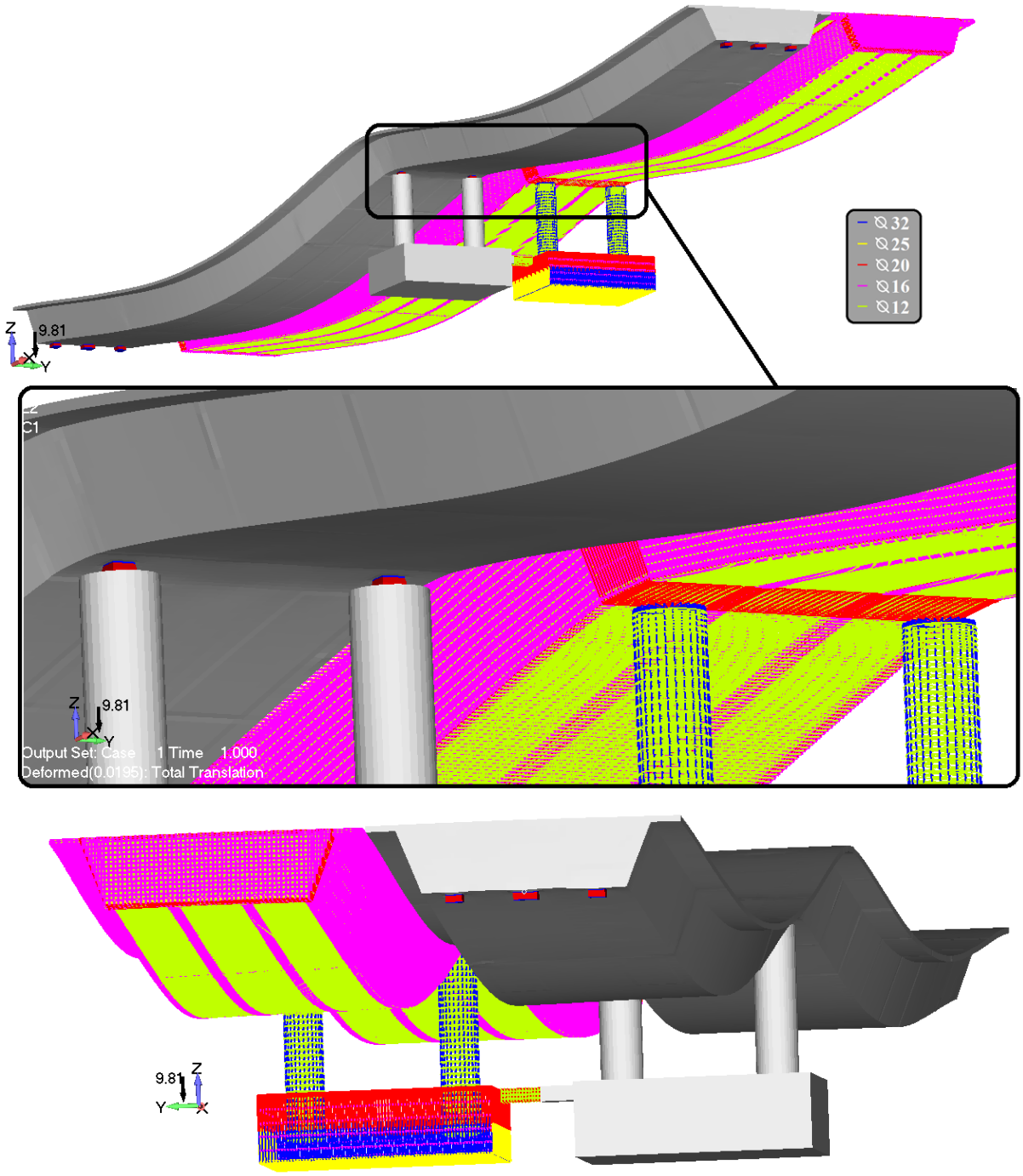

Figure 37. Double Deck RC Bridge. Deformed shape of the hexahedral and embedded rebar FE meshes.

In order to further investigate the computational performance of the under study method, the mesh of the RC Bridge was increased by 2. After the numerical analysis of the increased FE model, which consisted of 205,928 hexahedral concrete FEs and 95,082 embedded rebar macro-elements, the algorithm managed to generate 1,055,770 embedded rebar elements from which 2,878 had a length shorter than 5 mm and were excluded from the analysis procedure. The required computational time for the generation of the embedded rebar elements was 304 minutes and 5 seconds. The numerical investigation demonstrates the numerical efficiency of the under study numerical method.

Finally, it is important to state that modeling RC structures through the use of 3D detailed modeling that discretize the reinforcement grid with embedded rebar elements, has a drawback that relates to the construction of the embedded rebar macro-element mesh, especially in cases where the geometry of the structure has an irregular geometry. This procedure requires a significant effort which makes it prohibitive to be used for commercial purposes. So as to address this issue, an automatic mesh generation algorithm is required to be developed for generating the embedded rebar macro-element mesh inside the hexahedral elements in order to optimize (in terms of time) the embedded rebar macro-element mesh construction procedure.

5 ACKNOWLEDGEMENTS

The author would like to acknowledge the financial support from the Alhosn University of Abu Dhabi and the Vice Chancellor Prof. Abdul Rahim Sabouni for his support throughout this research work.

REFERENCES

[1] L. Jendele and J. Cervenka, On the solution of multi-point constraints – Application to FE analysis of reinforced concrete structures, *Computers and Structures*, **87**, 970–980, 2009.

[2] M.D. Kotsovos and M.N. Pavlovic, *Structural concrete. Finite Element Analysis for Limit State Design*, Thomas Telford: London, 1995.

[3] K.V. Spiliopoulos and G. Lykidis, An efficient three-dimensional solid finite element dynamic analysis of reinforced concrete structures, *Earthquake Engng Struct. Dyn.*, **35**, 137–157, 2006.

[4] H. Hartl, Development of a continuum mechanics based tool for 3d FEA of RC Structures and application to problems of soil-structure interaction, Ph.D. Thesis, Faculty of Civil Engineering, Graz Univ. of Technology, 2000.

[5] G. Markou, Detailed Three-Dimensional Nonlinear Hybrid Simulation for the Analysis of Full-Scale Reinforced Concrete Structures, Ph.D. Thesis, Institute of Structural Analysis and Seismic Research, National Technical University of Athens, 2011.

[6] V. Cervenka, *Large Deflections*, Cervenka Consulting, 2010.

[7] V.T. Hristovski and H. Noguchi, Finite Element Modeling of RC Members Subjected to Shear, *Third DIANA World Conference*, *Tokyo, Japan* 9-11 October 2002.

[8] G. Markou and M. Papadrakakis, An efficient generation method of embedded reinforcement in hexahedral elements for reinforced concrete simulations, *Advances in Engineering Software ADES*, **45**(1), 175-187, 2012.

[9] F. Barzegar and S. Maddipudi, Generating reinforcement in FE modeling of concrete structures, *Journal of Structural Engineering*, **120**, 1656 –1662, 1994.

[10] A.E. Elwi and T.M. Hrudey, Finite element model for curved embedded reinforcement, *Journal of Engineering Mechanics*, **115**, 740 –754, 1989.

[11] ASCE Task Committee on Concrete and Masonry Structures, *Finite element analysis of reinforced concrete*, ASCE, 1982.

[12] M.A.H. Abdel-Halim and T.M. Abu-Lebdeh, Analytical study of concrete confinement in tied columns, *Journal of Structural Engineering., ASCE*, **115**(11), 2810-2828, 1989.

[13] F. Gonzalez Vidosa, M.D. Kotsovos and M.N. Pavlovic, Three-dimensional finite element analysis of structural concrete, *Proc., Second Int. Conf. on Computer Aided Anal. and Des. of Concrete Struct.*, N. Bicanic, and H. Mang, eds., Vol. II, Pineridge Press, Swansea, Wales, 1029-1040, 1990.

[14] G. Markou, Embedded reinforcement mesh generation method for large-scale RC simulations: Case study, *AHU Journal of Engineering & Applied Sciences*, **5**(1), 23-42, 2012.

[15] Siemens P.L.M. Software, *World-class finite element analysis (FEA) solution for the Windows desktop*, Siemens Product Lifecycle Management Software Inc, 2009.